Proceedings of the 21st ICSMGE, Vienna, Austria, 14 – 19 June 2026. Pistrol, Adam & Schweiger (eds.)
Published by: ÖGG, Austrian Society for Geomechanics, Salzburg, Austria, ISBN 978-3-9503898-4-5
https://doi.org/10.53243/ICSMGE2026-1811

Stress-relaxation behavior in methane hydrate-bearing soils

Itai Bar, Aram Yakoby, Lior Rake, Shmulik Pinkert
Department of Civil and Environmental Engineering, Ben-Gurion University of the Negev, Beer-Sheva, Israel, pinkerts@bgu.ac.il

ABSTRACT: In recent years, there has been growing interest in methane hydrates due to their immense potential for gas production. These hydrates form within soil pore spaces under specific conditions of low temperature and high pressure and are commonly found in permafrost regions and beneath continental shelves. The geotechnical significance of hydrate-bearing soils arises from the substantial influence of the solid hydrates within the pore spaces on the soil's overall mechanical behavior. However, during gas production, this mechanical stability can be compromised due to hydrate dissociation processes. This study investigates the time-dependent mechanical behavior of methane hydrate-bearing sediments, a critical factor in understanding reservoir stability and optimizing gas extraction processes. Specifically, we focus on the viscous – stress relaxation and creep properties of hydrate-bearing soils through advanced laboratory experiments conducted on samples with methane hydrate artificially synthesized under controlled conditions. These experiments aim to examine the mechanical response of the soil-hydrate system, particularly under deviatoric loading and varied stress paths. The study is anchored in a robust theoretical framework, leveraging advanced mechanical modeling to interpret the findings. The evaluation of material properties and the parametric analysis provide valuable insights into the time-dependent behavior of sediments, potentially linking it to the inherent nanoscale instability of hydrates. The insights gained from this sample-scale investigation improve the engineering prediction of long-term deformation in gas production presses from hydrate reservoirs.

KEYWORDS: Methane hydrate-bearing soil, time-dependency, stress relaxation, geomechanics.

1 INTRODUCTION

Methane hydrates (MH) are crystalline compounds in which methane molecules are encaged within lattices of hydrogen-bonded water molecules. These solid hydrates are stable under thermodynamic conditions of high pressure and low temperature. Naturally, MH is typically found within the pore spaces of soils in two main environments: deep marine sediments, where high pressure dominates, and permafrost regions, where persistently low temperatures prevail. MH deposits are considered a major potential energy resource (Sloan & Koh, 2007), with recent estimates suggesting their energy content exceeds that of all known conventional fossil fuel reserves combined. Methane gas extraction from methane-hydrate-bearing sediments (MHBS) poses significant geomechanical challenge, such as gas production via depressurization or thermal stimulation, potentially destabilizing sediments (Boswell et al., 2017), and causing wellbore collapse. Understanding how MHBS respond to loading and deformation is essential for predicting wellbore integrity, slope stability, and long-term reservoir behavior. Therefore, a geomechanical understanding of MHBS is essential for the design and implementation of engineering processes related to gas extraction from these sediments.

The mechanical behavior of MHBS has been extensively investigated through laboratory testing. However, due to the complexity and high cost of obtaining undisturbed natural samples, most studies have focused on artificial MHBS specimens synthesized in controlled laboratory settings. Experimental results consistently show that mechanical properties are strongly influenced by hydrate saturation (S_h), defined as the volumetric fraction of hydrate relative to the pore volume. An increase in S_h is typically associated with higher shear strength, increased stiffness, and enhanced dilation behavior of the sediment (e.g., Hyodo et al., 2013; Masui et al., 2005; Pinkert & Grozic, 2016; Pinkert & Nadav, 2021). These effects are commonly attributed to hydrate-induced cohesion, stress-dilatancy mechanisms, and principles of effective stress-core concepts in geomechanics. In recent years, a range of constitutive models has been developed to capture these experimental findings, incorporating variables such as stress state, hydrate saturation, soil type, hydrate morphology, temperature effects, and more (e.g., Song et al., 2016; Dong et al., 2019; Santamarina & Rupple, 2010; Deusner et al., 2019; Pinkert & Grozic, 2014; Zhou et al., 2022; Rake & Pinkert 2024).

In addition to the extensively documented pseudo-static mechanical response of MHBS, its time-dependent behavior has emerged as a critical factor in assessing sediment stability during gas production. As gas is extracted from hydrate reservoirs, the stress state around the well evolves dynamically, making it increasingly challenging to maintain mechanical stability over time. Variations in extraction rate alter the stress application rate, potentially triggering time-dependent deformation processes. Understanding this dynamic behavior of MHBS is essential for ensuring safe and efficient gas recovery. To this aim, Triaxial tests with varying strain rates have been used to investigate the mechanical rate-effect of MHBS (e.g., Miyazaki, 2011, Miyazaki 2017, Deusner 2019). These studies consistently demonstrate that MHBS exhibits rate-dependent behavior. At high hydrate saturations, increased strain rates result in higher peak stress response and greater stiffness, indicating a strong coupling between deformation rate and the mechanical behavior. Conversely, hydrate-free sands show negligible sensitivity to strain rate, underscoring the distinct rheological characteristics introduced by hydrate presence.

Creep is another important time-dependent phenomenon, referring to progressive deformation under constant stress. During gas extraction, even if operations are paused and external loading remains constant, significant deformation may continue to develop over time. Experimental studies have shown that creep deformation in MHBS is influenced by temperature, confining pressure, and hydrate saturation (Miyazaki et al., 2011; Miyazaki et al., 2017; Li et al., 2019; Li et al.,2023). While hydrate-free samples typically follow a linear-logarithmic relationship between creep strain rate and time (Miyazaki et al., 2011; Li et al., 2023), hydrate-bearing samples often exhibit multiple creep stages (Miyazaki et al., 2011). Overall, the creep rate initially decreases logarithmically, and later exhibits an accelerated creep phase towards failure.

Time-dependent behavior of MHBS has also been observed at the molecular scale, although a direct link to macroscopic mechanical response remains unresolved. This study hypothesizes that macroscopic time-dependent

deformation originates from dynamic disequilibrium at the molecular level. This paper discusses this hypothesis and addresses it through experimental and analytical findings on the time-dependent behavior of MHBS. This paper discusses this hypothesis and addresses it through experimental and analytical findings on the time-dependent behavior of MHBS.

2 EXPERIMENTAL STUDY

The mechanical behavior of MHBS was studied using a high-pressure triaxial system with precise control of temperature, pore pressure, and confining stress (Figure 1). Cylindrical specimens (50 mm diameter, 100 mm height) were enclosed in a latex membrane and placed between heat-controlled end caps. Pore fluid (methane or water) was controlled via two high-precision piston pumps (20 MPa capacity), connected to an external gas supply. Confining pressure was applied through a double-wall cell, allowing independent control of inner and outer cells and enabling volume-change measurement. Temperature-control was achieved using a circulation system with internal tubing. The setup was mounted on a 100 kN load frame, with axial load and displacement monitored by internal and external sensors. Further system details are provided in Rake & Pinkert (2021).

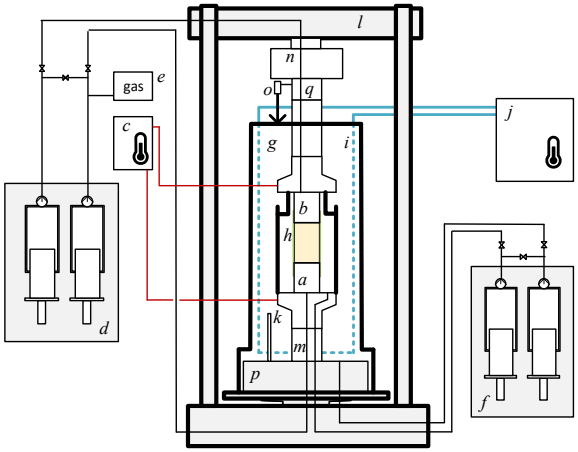

Figure 1. Schematic diagram of the temperature-controlled high-pressure triaxial system: (a-b) end caps, (c) cap heating, (d) pore pressure control, (e) gas inlet, (f) confining pressure control, (g-h) outer and inner cells, (i) thermal tubing, (j) circulation system, (k) thermometer, (l) load frame, (m-n) load cells, (o) LVDT, (p-q) thermal insulation.

The formation of MHBS samples was followed the excess-gas method: moist sand (7% water content) was prepared by mixing ice with frozen sand containing 2% fines, then compacted in layers into the specimen mold. The back-pressure was increase to 8 MPa through methane gas injection, while confining pressure was raised, reaching 9 MPa. Temperature was lowered to 3°C and maintained until gas consumption was stabilized (~48 h), indicating the completion of hydrate formation. Then, drained triaxial tests were conducted at a strain rate of 0.1%/min. Axial stress, strain, and volumetric change were continuously recorded. After reaching failure (>2 h), axial displacement was held constant, and stress relaxation was continuously monitored. Hydrate saturation was determined at the end of the test following the method in Rake & Pinkert (2021).

3 RESULTS

Figure 2 presents the deviatoric stress response with time throughout the entire test, under an effective confining stress of 1.2 MPa and a hydrate saturation of 42%. The test comprises two stages: (i) the shear phase, in which the sample is axially loaded at a constant strain rate of 0.1%/min, and (ii) the relaxation phase, initiated by halting axial displacement and allowing time-dependent stress relaxation to occur. As expected, during the first phase, the MHBS specimen exhibits higher stiffness and peak strength compared to the host-soil, and experiences a dramatic post-peak degradation, in agreement with previously reported mechanical trends. In the second phase, the MHBS samples experiences significant stress relaxation of 3.5 MPa (which is almost 50% of its deviatoric stress), while the host soil exhibits a minor stress relaxation of 0.7 MPa. The difference between the two residual stress responses of the MHBS and the host sand is hypothesized to be related to the volume of hydrate in the pore space.

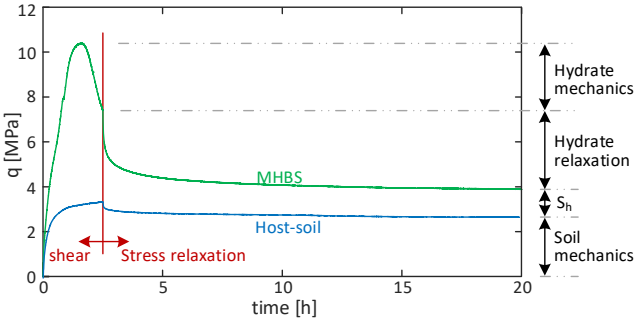

Figure 2. Triaxial compression response of MHBS and host-soil under an effective confining stress of 1.2 MPa and S_h = 42%. The test includes two phases: shear loading to peak strength under constant strain rate, followed by post-failure stress relaxation under constant axial displacement.

Figure 3 isolates the stress relaxation behavior observed during the second phase. Figure 3a shows the stress relaxation for MHBS, host-soil, and hydrate (inferred by subtracting the host-soil response from MHBS). The data is presented in terms of the normalized stress relaxation, from 0 to 100% stress convergence into the stress steady state. All three responses follow a similar decay trend. Notably, the relaxation timescale appears comparable for the hydrate-bearing and hydrate-free systems. Figure 3b presents the same data in terms of the decay in the deviatoric stress on a logarithmic time axis. In this representation, the MHBS, host-soil, and inferred hydrate response each exhibit an approximately linear trend, indicating logarithmic relaxation behavior with distinct slopes for each material.

4 ANALYSIS

In this work, we present an initial attempt to model the time-dependent behavior of hydrate as a viscous element within an analog mechanical model. For simplicity, we first applied the classical Maxwell model that is commonly used for describing stress relaxation, which consists of an elastic spring connected in series to a viscous damper, representing the response of the hydrate phase alone (isolated from the soil matrix). In this configuration, the spring stiffness is attributed to the hydrate saturation (S_h), while the damping action reflects the stress relaxation of the hydrate over time.

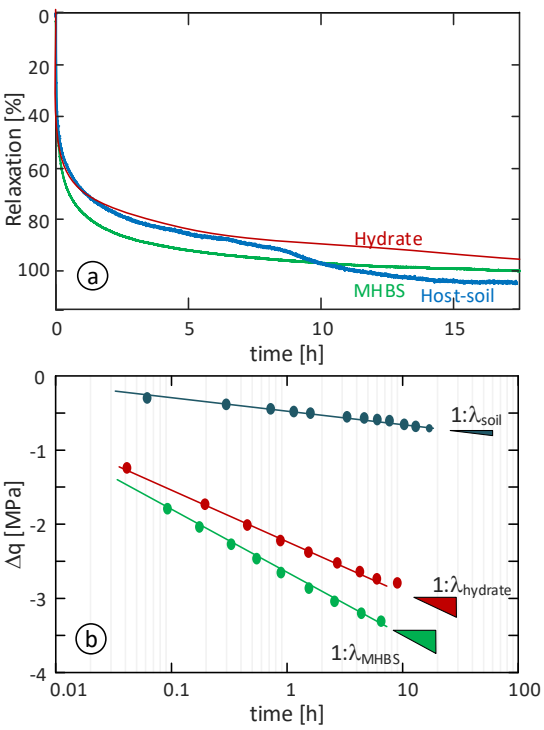

Figure 3. Stress relaxation behavior: (a) normalized stress relaxation curves for MHBS, host-soil, and inferred hydrate contribution, and (b) deviatoric stress relaxation plotted on a logarithmic time scale.

To capture the combined relaxation response of the composite material (hydrate and sand), we employed the Standard Four-Parameter Maxwell Model, illustrated in Figure 4. This model comprises two Maxwell elements—each a series connection of a spring (G) and damper (η)—assembled in parallel (Tschoegl, 1989). Such configuration enables the representation of two distinct relaxation processes that act concurrently, which we associate with the sand skeleton and the hydrate phase. The analytical representation of the analog model presented in Figure 4 is given by:

$$\Delta q(t) = \varepsilon_0 G_1 e^{-t/\tau_1} + \varepsilon_0 G_2 e^{t/\tau_2} - q_0 \qquad (1)$$

where $\tau_1 = \eta_1/G_1$, $\tau_2 = \eta_2/G_2$, ε_0 is the strain accumulated during shear, representing the starting strain for the relaxation phase, and q_0 is constant.

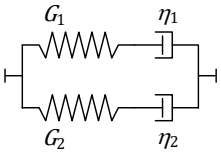

Figure 4. Schematic representation of the four-parameter Maxwell model applied to the analysis of time-dependent behavior in methane hydrate-bearing sediments (MHBS).

Figure 5 presents the experimentally obtained stress-relaxation curve, alongside the best-fit analytical solution and additional curves illustrating the model's sensitivity to parameter variations. The best-fit parameters characterizing the tested sample, extracted through nonlinear curve fitting, are also presented in the figure. These parameters define the stiffness and characteristic relaxation times of each mechanical branch, providing insights into the viscoelastic behavior of methane hydrate-bearing sediments under stress relaxation conditions.

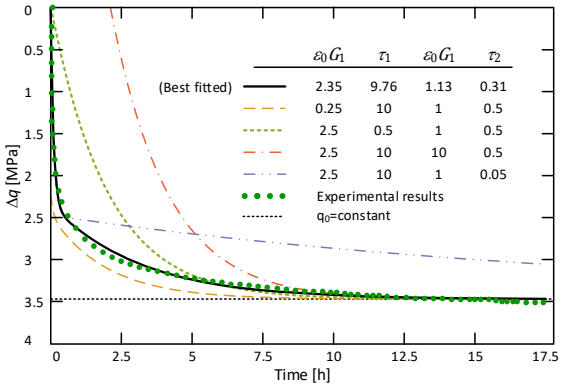

Figure 5. Model predictions compared to experimental data. Parameter sensitivity curves illustrate the influence of stiffness and relaxation times on the fitted response. q0 = 3.49 MPa for all curves.

5 DISCUSSION

Although methane hydrates are considered stable under global thermodynamic conditions, recent molecular dynamics simulations reveal that this stability does not necessarily persist at the molecular scale (Wu et al., 2015; Chen et al., 2022). The research hypothesizes that the apparent contradiction between macroscopic stability and molecular-scale instability can be reconciled by introducing the dimension of time. That is, molecular-scale instabilities occurring in real time may manifest at larger spatial scales only after a certain period. In other words, the larger the geometric scale, the more time is required for the effects of such microscopic instabilities to become evident. Practically speaking, in a granular soil system containing hydrate within its pores, the molecular restructuring of the hydrate is expected to evolve into a geometry that aligns with the prevailing stress or strain state in the soil, in accordance with the system's tendency toward minimum energy. To illustrate this concept, Figure 6 presents a qualitative demonstration of how hydrate restructuring affects mechanical measurements. Figure 6a depicts a scenario in which the applied load remains constant, while the system undergoes a gradual volume reduction—resembling a creep-like process. Figure 6b illustrates a scenario where the volume is held constant, while stress relaxation occurs over time.

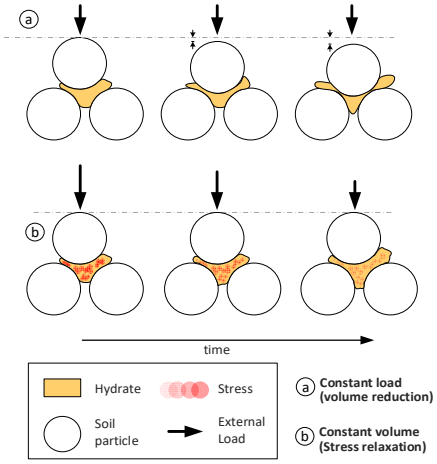

Figure 6. Schematic illustration of the hydrate restructuring effect, via either (a) stress-controlled or (b) strain-controlled scenarios.

The experiments in this work align with the demonstration in Figure 6b, where the volume is also held constant and stress relaxation occurs, attributed to the hypothesized molecular-scale hydrate restructuring. The four-parameter Maxwell model (Figure 4) was selected over the classic Maxwell model, where elements are connected in series, because the observed relaxation curve reflects the combined response of hydrate and soil. The initial rapid stress reduction is attributed to hydrate restructuring, while the subsequent gradual decay corresponds to the relaxation response of the soil skeleton.

6 CONCLUSIONS

This study presents a hypothesis linking the time-dependent mechanical behavior of methane hydrate-bearing sediments to the phenomenon of local instability experienced by the hydrate at the molecular scale. The time-dependent mechanical response was demonstrated through a triaxial shear test on hydrate-bearing soil, where, after reaching failure, deformation was held constant and stress relaxation was observed.

An initial analytical model was presented to quantify this behavior over time, focusing on the hydrate phase within the sample. For future research, we recommend further development of the model, guided by additional experimental data that examine the influence of parameters such as varying hydrate saturation (S_h), confining stress, and temperature. The current model characterizes the behavior of a viscous material (Tschoegl, 1989), and was therefore suitable for capturing the relaxation phenomenon. However, additional elements may be required to fully represent the solid-like characteristics of the composite.

7 ACKNOWLEDGEMENTS

This research was partly funded by the Israel Ministry of Energy through the program for funding studies in the energy and earth sciences; contract #222-17-003. We thank Mr. Dmitri Mazankin and Mr. Haim Feldman for their dedicated technical assistance.

8 REFERENCES

Boswell, R., Collett, T.S., Myshakin, E., Ajayi, T., & Seol, Y. (2017). The increasingly complex challenge of gas hydrate reservoir simulation. In Proceedings of the 9th International Conference on Gas Hydrates, Denver, Colorado, 25–30 June 2017.

Chen, Y., Sun, C., Wang, Y., & Zhang, Y. (2022). Time-dependent behavior of methane hydrate at the molecular scale. Journal of Physical Chemistry C, 126(3), 1643–1651.

Deusner, C., Gupta, S., Xie, X.G., Leung, Y.F., Uchida, S., Kossel, E., & Haeckel, M. (2019). Strain rate-dependent hardening-softening characteristics of gas hydrate-bearing sediments. Geochemistry, Geophysics, Geosystems, 20(11), 4885–4905.

Dong, L., Li, Y., Liao, H., Liu, C., Chen, Q., Hu, G., Liu, L., & Meng, Q. (2020). Strength estimation for hydrate-bearing sediments based on triaxial shearing tests. Journal of Petroleum Science and Engineering, 184, 106478.

Hyodo, M., Li, Y., Yoneda, J., Nakata, Y., Yoshimoto, N., Nishimura, A., & Song, Y. (2013). Mechanical behavior of gas-saturated methane hydrate-bearing sediments. Journal of Geophysical Research: Solid Earth, 118, 5185–5194.

Li, Y., Cheng, Y., Yan, C., Wang, Z., & Song, L. (2023). Triaxial creep tests and the visco-elastic-plastic constitutive model of hydrate formations. Gas Science and Engineering, 115, 205006.

Li, Y., Wu, P., Sun, X., Liu, W., Song, Y., & Zhao, J. (2019). Creep behaviors of methane hydrate-bearing frozen sediments. Energies, 12(2), 251.

Masui, A., Haneda, H., Ogata, Y., & Aoki, K. (2005). The effect of saturation degree of methane hydrate on the shear strength of synthetic methane hydrate sediments. In Proceedings of the Fifth International Conference on Gas Hydrates, Trondheim, Norway, 13–16 June 2005.

Miyazaki, K., Masui, A., Sakamoto, Y., Aoki, K., Tenma, N., & Yamaguchi, T. (2011). Triaxial compressive properties of artificial methane-hydrate-bearing sediment. Journal of Geophysical Research: Solid Earth, 116, B06102.

Miyazaki, K., Tenma, N., & Yamaguchi, T. (2017). Relationship between creep property and loading-rate dependence of strength of artificial methane-hydrate-bearing Toyoura sand under triaxial compression. Energies, 10, 1466.

Miyazaki, K., Yamaguchi, T., Sakamoto, Y., & Aoki, K. (2011). Time-dependent behaviors of methane-hydrate bearing sediments in triaxial compression test. International Journal of the JCRM, 7(1), 43–48.

Pinkert, S., & Grozic, J.L.H. (2014). Prediction of the mechanical response of hydrate-bearing sands. Journal of Geophysical Research: Solid Earth, 119(6), 4695–4707.

Pinkert, S., & Grozic, J.L.H. (2016). Experimental verification of a prediction model for hydrate-bearing sand. Journal of Geophysical Research: Solid Earth, 121, 4147–4155.

Pinkert, S., & Nadav, D. (2021). Analytical-Empirical approach for estimating kinematic-response relationships between hydrate-bearing soils and standard soils. *Journal of Geotechnical and Geoenvironmental Engineering*, 147(1), Article 04020148.

Rake, L., & Pinkert, S. (2021). The 'excess gas' method for laboratory formation of methane hydrate-bearing sand: geotechnical application. Scientific Reports, 11, 22068.

Rake, L., & Pinkert, S. (2024). The effect of hydrate formation conditions on the mechanics of laboratory methane hydrate-bearing sediments. Journal of Geophysical Research: Solid Earth, 129(10), e2024JB029217.

Santamarina, J.C., & Ruppel, C. (2010). The impact of hydrate saturation on the mechanical, electrical, and thermal properties of hydrate-bearing sand, silts, and clay. In Geophysical Characterization of Gas Hydrates, Society of Exploration Geophysicists, 373–384.

Sloan, E.D. Jr., & Koh, C.A. (2007). Clathrate Hydrates of Natural Gases (3rd ed.). Boca Raton: CRC Press.

Song, Y., Zhu, Y., Liu, W., Li, Y., Lu, Y., & Shen, Z. (2016). The effects of methane hydrate dissociation at different temperatures on the stability of porous sediments. Journal of Petroleum Science and Engineering, 147, 77–86.

Tschoegl, N.W. (1989). The Phenomenological Theory of Linear Viscoelastic Behavior. Springer.

Wu, D., Zhang, Y., & Wang, J. (2015). A molecular dynamics study on the mechanical properties of methane hydrate. Physical Chemistry Chemical Physics, 17(27), 18070–18077.

Zhou, B., Sanchez, M., Oldecop, L., & Santamarina, J.C. (2022). A geomechanical model for gas hydrate bearing sediments incorporating high dilatancy, temperature, and rate effects. Energies, 15(12), 4280.